New Constraint for Isotropic Lorentz Violation from LHC Data

David Amram,[1,*] Killian Bouzoud,[2,†] Nicolas Chanon,[1,‡] Hubert Hansen,[1,§]
Marcos R. Ribeiro, Jr.,[3,‖] and Marco Schreck[4,¶]

[1]*Université de Lyon, Université Claude Bernard Lyon 1, CNRS/IN2P3, IP2I Lyon, UMR 5822, Villeurbanne, France*
[2]*SUBATECH, Nantes Université, IMT Atlantique, IN2P3/CNRS, 4 rue Alfred Kastler, La Chantrerie BP 20722, 44307 Nantes, France*
[3]*Instituto de Física, Universidade de São Paulo, Cidade Universitária, São Paulo (SP), 05508-090, Brazil*
[4]*Departamento de Física, Universidade Federal do Maranhão, Campus Universitário do Bacanga, São Luís (MA), 65085-580, Brazil*

(Received 22 December 2023; accepted 10 April 2024; published 20 May 2024)

New calculations for the kinematics of photon decay to fermions *in vacuo* under an isotropic violation of Lorentz invariance (LV), parametrized by the standard-model extension, are presented in this Letter and used to interpret prompt photon production in LHC data. The measurement of inclusive prompt photon production at the LHC Run 2, with photons observed up to a transverse energy of 2.5 TeV, provides the lower bound $\tilde{\kappa}_{tr} > -1.06 \times 10^{-13}$ on the isotropic coefficient $\tilde{\kappa}_{tr}$ at 95% confidence level. This result improves over the previous bound from hadron colliders by a factor of 55. The calculations for the kinematics of photon decay have further potential use to constrain LV coefficients from the appearance of fermion pairs.

DOI: 10.1103/PhysRevLett.132.211801

Introduction.—Considering the technology and experimental capabilities of the early 21st century, it is impossible to probe quantum gravity directly, since experiments would require particles whose energies lie in the vicinity of the Planck scale. Such energies are indispensable to resolve structures of the smallest length scales imaginable such as strings or a spacetime foam [1,2]. Fortunately, there are alternatives to observing quantum gravity phenomena in a direct way. To do so, we resort to the two most successful theories: the standard model (SM) of elementary particles and general relativity (GR). The first is based on global Lorentz invariance, whereby GR is governed by diffeomorphism symmetry as well as local Lorentz invariance. It is these symmetries that play a crucial role in the quest for quantum gravity effects.

The SM and GR describe particles and gravity astoundingly well for energies much lower than the Planck scale. A valuable approach to quantum gravity phenomenology consists in searching for tiny deviations from these established theories. In the framework of effective field theory, there are several possibilities of how to proceed. First, the SM is extended by excitations of new degrees of freedom described by non-SM fields. Second, contributions are introduced that preserve the symmetries of the SM and GR, but involve higher-order derivatives. Third, an alternative is to consider violations of at least one of the fundamental spacetime symmetries. Our interest lies on the latter approach.

The gravitational field can be neglected for our purpose, which means that we will focus on violations of global Lorentz invariance. Such effects are motivated by a set of articles indicating a breakdown of Lorentz symmetry in string field theory [3–7], loop quantum gravity [8,9], noncommutative field theory [10,11], spacetime foam models [12–14], chiral field theories defined in spacetimes with nontrivial topologies [15–17], and Hořava-Lifshitz gravity [18]. A comprehensive technique established for a broad program of experimental searches for Lorentz violation (LV) is to use a model-independent effective parametrization of deviations from Lorentz symmetry, which the standard-model extension (SME) [19,20] provides. The latter respects the gauge symmetry and particle content of the SM. Lorentz violation is parametrized by tensor-valued background fields whose components, which are denoted as controlling coefficients, describe the amount of symmetry violation. These background fields are coupled to the SM fields such that the resulting terms are invariant with respect to coordinate boosts and rotations. Within effective field theory, *CPT* violation was shown to imply a violation of Lorentz symmetry [21], which is why *CPT*-violating operators are also contained in the SME.

In the SME, particles obey modified dispersion relations and processes are described perturbatively by a set of modified Feynman rules [22–24]. The modified kinematics may enable unusual processes that are forbidden in the SM due to energy-momentum conservation. For example,

under certain conditions, a fermion subject to LV can lose energy by the emission of photons. This process is reminiscent of Cherenkov radiation in optical media with the crucial difference that it occurs *in vacuo*. Therefore, the latter is called vacuum Cherenkov radiation [25–49]. Another prominent process is photon decay into a fermion–antifermion pair [35,36,39,50–69], which the focus is on in this Letter.

Photon decay can occur in the *CPT*-even photon sector of the SME that is governed by 19 independent controlling coefficients [20,70,71]. Ten of these imply vacuum birefringence and are strongly constrained by spectropolarimetry measurements [70,72–77]. The remaining 9 coefficients are nonbirefringent at first order in LV. A subset of 8 leads to anisotropic photon propagation and a single one describes LV effects that are spatially isotropic. Searches for anisotropic effects via small-scale laboratory experiments have provided a large number of tight bounds on such coefficients [78–81], whereas astroparticle physics has led to competitive constraints on the isotropic coefficient [36,39,49,68] (cf. Table D16 in Ref. [82]).

When it comes to particle energy and propagation distance, astroparticle physics experiments have an advantage over collider experiments in constraining LV. The highest energies of astrophysical photons detected lie in the ballpark of few hundred TeV [66] to 2.5 PeV, as observed by LHAASO [83,84]. However, the drawback of astroparticle experiments is that the interpretation relies on models, e.g., for the distribution of sources and the injection of nuclei through the source environment [85]. These are necessary to describe the energy spectrum, composition, and arrival direction of astroparticles [65]. In addition, information related to the intrinsic spectrum of the source, its evolution, and emission mechanism is not necessarily available [67,86,87]. By contrast, Earth-based laboratory experiments provide a reproducible, controlled source of prompt photons, well understood in term of the SM predictions, leading to limits on LV that can be considered as less model dependent and, hence, more conservative. Such collider bounds are complementary to astrophysical constraints. In this work we will demonstrate how prompt photons measured at the LHC are capable of improving the constraint on isotropic *CPT*-even LV by a factor larger than 50, in comparison with the present limit derived at the Tevatron.

Minimal-SME photon sector.—We consider a modified quantum electrodynamics with LV in the photon sector, but standard Dirac fermions:

$$S = \int \mathrm{d}^4x \left[-\frac{1}{4}(\eta^{\mu\varrho}\eta^{\nu\sigma} + \kappa^{\mu\nu\varrho\sigma}) F_{\mu\nu}(x) F_{\varrho\sigma}(x) + \frac{1}{2}\bar{\psi}(x)(\gamma^\mu \mathrm{i} D_\mu - m_f)\psi(x) + \mathrm{H.c.} \right], \tag{1}$$

with the electromagnetic field strength tensor $F_{\mu\nu} = \partial_\mu A_\nu - \partial_\nu A_\mu$ of the $U(1)$ gauge field A_μ. Furthermore, ψ is a Dirac spinor field and $\bar{\psi} \equiv \psi^\dagger \gamma^0$ the corresponding Dirac conjugated field. All fields are defined in Minkowski spacetime with metric $\eta_{\mu\nu}$ of signature $(+,-,-,-)$. We employ the standard Dirac matrices satisfying the Clifford algebra $\{\gamma^\mu, \gamma^\nu\} = 2\eta^{\mu\nu}$ and m_f is the fermion mass. The Dirac field is minimally coupled to the gauge field via the covariant derivative $D_\mu = \partial_\mu + \mathrm{i}qA_\mu$ with the fermion charge q. The violation of Lorentz invariance is parametrized via $\kappa^{\mu\nu\varrho\sigma}$, which transforms as a four-tensor of rank 4 under coordinate boosts and rotations, but remains fixed with respect to boosts and rotations of experiments proper. The object $\kappa^{\mu\nu\varrho\sigma}$ implies preferred spacetime directions leading to a boost- and/or direction-dependent form of the laws of physics.

The physics of Eq. (1) is described by a nontrivial refractive index of the vacuum that leads to a speed of light different from the maximum velocity of Dirac particles. The refractive index may be anisotropic or even polarization dependent resulting in vacuum birefringence. Since the latter effect is tightly constrained at the level of 10^{-34} to 10^{-35} by spectropolarimetry measurements [82], we discard the birefringent part of $\kappa^{\mu\nu\varrho\sigma}$ involving 10 coefficients. The remaining 9 coefficients are parametrized by the nonbirefringent *ansatz* [32]:

$$\kappa^{\mu\nu\varrho\sigma} = \frac{1}{2}(\eta^{\mu\varrho}\tilde{\kappa}^{\nu\sigma} - \eta^{\mu\sigma}\tilde{\kappa}^{\nu\varrho} + \eta^{\nu\sigma}\tilde{\kappa}^{\mu\varrho} - \eta^{\nu\varrho}\tilde{\kappa}^{\mu\sigma}), \tag{2}$$

where $\tilde{\kappa}^{\mu\nu}$ is a symmetric and traceless (4×4) matrix. We study isotropic LV in the laboratory frame, which is the simplest choice for a first analysis before investigating more intricate cases. There is a single coefficient usually denoted as $\tilde{\kappa}_{\mathrm{tr}}$ that parametrizes isotropic LV in the theory of Eq. (1). The coefficients of the matrix $\tilde{\kappa}^{\mu\nu}$ are then chosen as

$$\tilde{\kappa}^{\mu\nu} = \frac{3}{2}\tilde{\kappa}_{\mathrm{tr}} \mathrm{diag}\left(1, \frac{1}{3}, \frac{1}{3}, \frac{1}{3}\right)^{\mu\nu}. \tag{3}$$

Thus, the dispersion relation for photons is modified and reads

$$\omega = \mathcal{A}|\mathbf{k}|, \qquad \mathcal{A} = \sqrt{\frac{1-\tilde{\kappa}_{\mathrm{tr}}}{1+\tilde{\kappa}_{\mathrm{tr}}}}, \tag{4}$$

where $\mathbf{k}$ is the three-momentum of the photon. The isotropy of the result is evident. Since the phase and group velocities of photons obey

$$v_{\mathrm{ph}} \equiv \frac{\omega}{|\mathbf{k}|} = \mathcal{A}, \qquad v_{\mathrm{gr}} \equiv |\boldsymbol{\nabla}_{\mathbf{k}}\omega| = \mathcal{A}, \tag{5}$$

there is no vacuum dispersion. For $\tilde{\kappa}_{\mathrm{tr}} \in (0,1]$ we have that $v_{\mathrm{gr}} < 1$. The dispersion relation of Dirac fermions is the standard one for massive particles. Hence, the latter can

possibly propagate faster than light. For $\tilde{\kappa}_{tr} \in (-1, 0)$ we observe that $v_{gr} > 1$ and photons always move faster than fermions, no matter what their energy.

In the first kinematic regime, vacuum Cherenkov radiation can occur, whereas photon decay *in vacuo* is a characteristic process for the second regime. Both processes are governed by thresholds, i.e., they occur if the energy of the initial particle exceeds a certain minimum that depends on the fermion mass and the controlling coefficient. Since vacuum Cherenkov radiation with LV in photons and fermions, respectively, has already been studied exhaustively [25–33,35–48], we intend to investigate photon decay. Thus, in what follows, we will take $\tilde{\kappa}_{tr} \in (-1, 0)$.

Kinematics and dynamics of photon decay.—Now, let us look at the basics of photon decay $\gamma \to f\bar{f}$ within the isotropic sector of Eq. (1). The threshold energy E^{th} of the incoming photon is best computed by considering the three-momenta of all particles as collinear. Energy-momentum conservation then implies [36]

$$E^{th} = 2m_f \sqrt{\frac{1-\tilde{\kappa}_{tr}}{-2\tilde{\kappa}_{tr}}}. \tag{6}$$

Several observations are in order. First, for a massless fermion, the process occurs without a threshold. Second, the expression is real only for $\tilde{\kappa}_{tr} < 0$, whereupon photon decay is forbidden for $\tilde{\kappa}_{tr} > 0$. Third, the threshold goes to infinity for $\tilde{\kappa}_{tr} \mapsto 0$, since the process is energetically not allowed when Lorentz symmetry is intact. Fourth, since the threshold is proportional to the particle mass, further decay channels into more massive fermion-antifermion pairs open up for rising photon energy.

The total decay width Γ of photon decay for the isotropic sector was already obtained in Ref. [36]. Instead, what we will need in the forthcoming analysis are different quantities, which have not been reported in the literature, so far. If the incoming-photon energy exceeds the threshold, the surplus in energy is used to provide a nonzero angle θ between the three-momenta of the final-state particles. The latter reads

$$\cos\theta = \frac{E_f(E_\gamma - E_f) + \frac{\tilde{\kappa}_{tr}}{1-\tilde{\kappa}_{tr}} E_\gamma^2 + m_f^2}{\sqrt{[E_f^2 - m_f^2][(E_\gamma - E_f)^2 - m_f^2]}}, \tag{7}$$

where E_γ and E_f are the energies of the incoming photon and outgoing fermion, respectively. The energy of the outgoing antifermion is determined by energy-momentum conservation. Furthermore, the partial decay width with respect to the energy of the final fermion can be cast into the form

$$\frac{d\Gamma}{dE_f} = \frac{\alpha}{(1+\tilde{\kappa}_{tr})^2 \sqrt{1-\tilde{\kappa}_{tr}^2} E_\gamma^2} \times \left\{(1-\tilde{\kappa}_{tr})[2\tilde{\kappa}_{tr} E_f(E_\gamma - E_f) + (1+\tilde{\kappa}_{tr}) m_f^2] - \tilde{\kappa}_{tr} E_\gamma^2\right\}, \tag{8}$$

with the fine-structure constant $\alpha = e^2/(4\pi)$. Equations (7) and (8) are new results. Evaluating the final-particle phase space, the fermion energy lies within the following interval of a minimum and maximum energy:

$$E_f \in [E_{min}, E_{max}], \tag{9a}$$

$$E_{min} = \frac{1}{2}(E_\gamma - \bar{E}), \qquad E_{max} = \frac{1}{2}(E_\gamma + \bar{E}), \tag{9b}$$

$$\bar{E} \equiv \sqrt{\frac{1+\tilde{\kappa}_{tr}}{1-\tilde{\kappa}_{tr}}\left[E_\gamma^2 + 2\left(\frac{1}{\tilde{\kappa}_{tr}} - 1\right) m_f^2\right]}. \tag{9c}$$

The angle of Eq. (7) is well defined only when E_f lies in the interval set by Eq. (9).

Search for photon decay to electrons in vacuo at the LHC.—The proton-proton collisions at the LHC are providing a large sample of high-E_T^γ prompt photons (where E_T^γ is their transverse energy). In this section, we reinterpret in the context of a possible LV the distribution of the differential cross section $d\sigma/dE_T^\gamma$ of inclusive prompt photons, which was measured with the ATLAS detector at a center-of-mass energy of $\sqrt{s} = 13$ TeV [88]. This analysis, performed with an integrated luminosity of 36.1 fb^{-1} at the LHC run 2, reports photons with the largest E_T^γ observed at the LHC, binning up to 2.5 TeV for photon pseudorapidity $|\eta^\gamma| < 0.6$. The latter provides an improvement as compared to a previous result of the CMS experiment, with photons of up to 2 TeV [89].

Here, we make the hypothesis that photons can decay into e^+e^-. In the following, models are built for E_T^γ distributions, based on the hypothesis of LV signals and SM backgrounds. Events of the process $pp \to \gamma + \text{jet}$ at tree-level with up to 3 additional partons at leading order in perturbative QCD and matched with parton showers are simulated with the SHERPA generator v.2.2.15 [90,91]. The events are further reweighted using tables from HEPData [92] such that no difference remains in the E_T^γ distribution between the SHERPA sample used in this article and the SHERPA sample employed in the ATLAS paper [88]. The events are selected using RIVET [93], a framework providing publicly available codes for the analysis of parton-shower level Monte Carlo (MC) events. We require $E_T^\gamma > 125$ GeV within the acceptance region $|\eta^\gamma| < 0.6$, with criteria on photon isolation taken from the RIVET routine corresponding to those of a similar analysis performed at 8 TeV [94]. Note that the same criteria are employed in the 13 TeV analysis [88].

For each event passing the selection, the photon with the largest E_T^γ is selected. Under the hypothesis of a nonzero $\tilde{\kappa}_{tr}$, the probability for photons to reach the ATLAS detector is computed as $e^{-\Gamma x}$, using the total photon decay width Γ, which follows from integrating Eq. (8). Moreover, we assume a distance of 33 mm between the interaction point

and the closest layer of the ATLAS pixel detector [95] at LHC run 2. As already noted [35], the photon decay process is very efficient, since only 0.038% of the photons do not decay over this distance, above the threshold $E^{\rm th} = 2$ TeV. If photons decay, distributions based on Eqs. (7) and (9) are used to generate the fermion and antifermion four-momenta, employing uniform distributions in azimuths.

Since the electrons arising from photon decay *in vacuo* can be reconstructed within the detector, it must be verified whether or not they would still be identified as photons. The e^+e^- system can be reconstructed as one-leg or two-leg converted photons, or as electrons. Reference [88] reports an uncertainty of approximately 1.5% on photon identification, which we take as an estimate of the probability for an electron to be reconstructed as a photon. If one electron is reconstructed as a photon, the value of its transverse energy, drawn according to the probability density $d\Gamma/dE_f$, is included in the distribution of E_T^γ. If two electrons are reconstructed as a photon, the largest transverse energy is included in the distribution of E_T^γ. Among the photons within a E_T^γ bin, a fraction of about 3% would be recovered from the decay into e^+e^- as reconstructed photons with a lower E_T^γ value. The procedure described above provides models for the E_T^γ distribution of SM prompt photon production (treated as a background), and of a SM contribution with LV (treated as a signal) under any hypothesis for the value of $\tilde{\kappa}_{\rm tr}$. These can be compared to the spectrum of E_T^γ measured with the ATLAS detector. Predictions are shown in Fig. 1 for several values of the threshold energy.

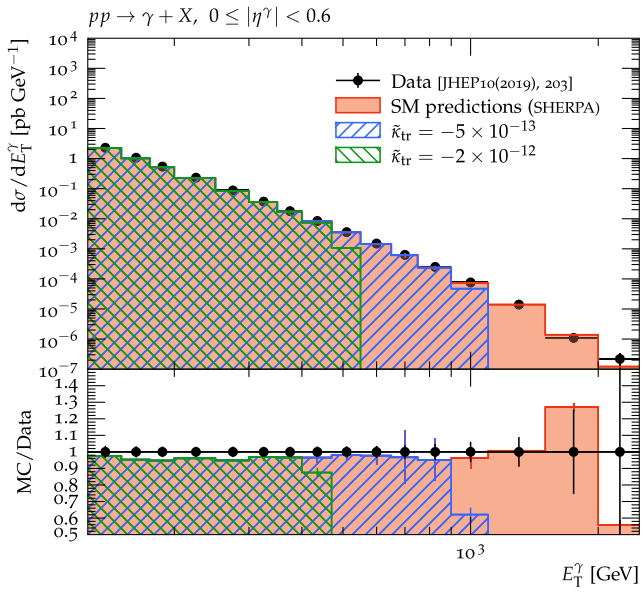

FIG. 1. Differential cross section for inclusive prompt photon production measured with the ATLAS detector [88], compared with the predictions from the SHERPA generator assuming several energy thresholds for photon decay *in vacuo*.

The statistical treatment employed to extract bounds on $\tilde{\kappa}_{\rm tr}$ uses the modified frequentist CL_s method [96], based on the likelihood ratio of the SM + LV hypothesis against the SM-only hypothesis, assuming the number of events are Poisson distributed in each bin. The central value for the number of events N_i is computed from the differential cross sections $d\sigma_i/dE_T^\gamma$ in each bin i as

$$N_i = \frac{d\sigma_i}{dE_T^\gamma} \cdot \Delta E_{T,i}^\gamma \cdot \epsilon \cdot L, \tag{10}$$

where $\Delta E_{T,i}^\gamma$ is the bin width, ϵ the efficiency of photon reconstruction and identification, and L is the integrated luminosity. The systematic uncertainties in the ATLAS measurement, which impact the predictions for the models, are from multiple sources: background subtraction, unfolding of the detector effect, pileup, trigger and photon selection efficiencies, photon energy scale, and resolution. Other uncertainties considered are the MC statistical uncertainty in the SHERPA sample, as well as the theory uncertainties quoted for the ATLAS sample, arising from QCD renormalization and factorization scale, the parton distribution functions, strong coupling constant α_s, and the parton shower. The values of the systematic uncertainties are added in quadrature in each bin, and treated conservatively as a separate Gaussian nuisance parameter for each bin of the E_T^γ distribution. The total systematic uncertainty ranges from 2.3% at low values of E_T^γ to 7.6% at high values.

The achieved bound on $\tilde{\kappa}_{\rm tr}$ as a function of the CL_s criterion is shown in Fig. 2. The conventional criterion of $CL_s < 0.05$ is employed, leading to the following limit at 95% confidence level on the allowed region:

$$\tilde{\kappa}_{\rm tr} > -1.06 \times 10^{-13}. \tag{11}$$

This corresponds to a threshold energy of $E^{\rm th} = 2.218$ TeV. The bound quoted above represents a large improvement, of a factor of ≈55, over the previous bound $\tilde{\kappa}_{\rm tr} > -5.8 \times 10^{-12}$ [35]. The latter was set by reinterpreting D0 prompt photon data [97] where the last E_T^γ bin was measured up to 340 GeV. The order of magnitude of the improvement can be understood, since the LV/SM separation is the largest in the last bin, reporting photons with the largest energy, and recalling that $\tilde{\kappa}_{\rm tr} \propto (m_f/E^{\rm th})^2$ according to Eq. (6). As a matter of fact, assuming conservatively that the largest energy observed is set by the left-hand side boundary of the last measured bin, i.e., 2 TeV, and that it corresponds to $\eta^\gamma = 0$, fixes the minimum threshold to $E^{\rm th} \approx 2$ TeV.

By assuming that all of the higher-energy photons decay immediately, this in turn provides a qualitative bound $\tilde{\kappa}_{\rm tr} > -1.3 \times 10^{-13}$. It should be noted that this method leads to a qualitative estimate only, since it does not include systematic uncertainties, and neither considers the probability of photons to survive up to the detector nor the

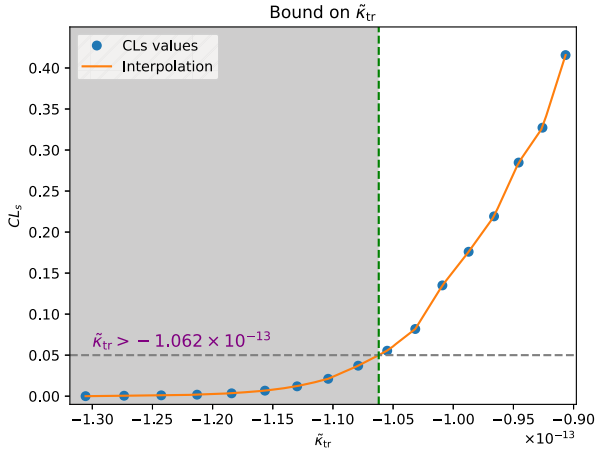

FIG. 2. Bound on $\tilde{\kappa}_{tr}$ as a function of the CL_s value. A bound with a 95% confidence level is defined by the region $CL_s < 0.05$.

probability of the e^+e^- system to be reconstructed as a photon. The improvement of Eq. (11) by nearly 20% over this simple estimate arises from the statistical method employed, which makes full use of the statistical power of the last E_T^γ bin. It is instructive to check the result without any systematic uncertainties, in which case the bound achieved would be $\tilde{\kappa}_{tr} > -1.045 \times 10^{-13}$. The result in Eq. (11) is dominated by the statistical uncertainties in the data.

An upper bound $\tilde{\kappa}_{tr} < 1.2 \times 10^{-11}$ was set from the LEP beam energy stability being interpreted as showing no evidence for vacuum Cherenkov radiation from electrons [35]. Such a limit cannot be improved by referring to the LHC beam stability, since the LHC collides protons. The SuperKEKB facility [98] is nowadays colliding e^+ and e^-, but does so at a lower center-of-mass energy than at LEP, which still provides the best results. Future particle colliders like the FCC-ee would collide electrons of 183 GeV [99] providing upper bounds improved by a factor of 3. The FCC-hh [100] is planned to collide 100 TeV protons; assuming that prompt photons of ≈20 TeV would be produced, the lower bound would improve by 2 orders of magnitude over the results presented previously.

Conclusions.—This Letter provides a new evaluation of the kinematics of photon decay into fermions *in vacuo* under an isotropic violation of Lorentz invariance. These results were used to reinterpret a measurement of inclusive prompt photon production at the LHC run 2, with photons observed up to a transverse energy of 2.5 TeV. A new bound on the isotropic SME coefficient $\tilde{\kappa}_{tr}$ was set from LHC data, arising from the absence of an observation of photon decay to electrons *in vacuo*. The limit yields $\tilde{\kappa}_{tr} > -1.06 \times 10^{-13}$ at 95% confidence level, a result that is approximately 55 times more stringent than a previous bound extracted from Tevatron data. The calculations for the kinematics of photon decay could be used in the future to bound LV coefficients from the appearance of fermion pairs.

M. S. greatly acknowledges support via the grants FAPEMA Universal 00830/19 and CNPq Produtividade 310076/2021-8. Furthermore, M. S. is indebted to CAPES/Finance Code 001.

Appendix: Photon decay to top quarks.—As an additional illustration of Eqs. (6)–(9), we focus on top quarks, assuming a mass $m_t = 172.5$ GeV. We highlight the difference between the kinematics of photon decay to top-quark pairs relative to that of SM $pp \to t\bar{t}$ processes. In this setting, the parameter $\tilde{\kappa}_{tr}$ must be replaced by a combination of photon and top-quark coefficients [35], $\tilde{\kappa}_{tr} - (4/3)c_t^{TT}$. Besides, as c_t^{TT} is an isotropic coefficient in the quark sector where constraints are weak compared to those for $\tilde{\kappa}_{tr}$ [82], we can neglect $\tilde{\kappa}_{tr}$ in the following. The coefficient c_t^{TT} induces a shift in the cross section for the process $pp \to t\bar{t}$, which would likely be attributed to a QCD effect [101,102].

However, top pairs produced from photon decay would entail a different kinematics, which is illustrated in Fig. 3 via the opening angle between top quarks for several threshold energies. This finding could be employed to set bounds on c_t^{TT}. It was checked that the azimuthal difference between top quarks shows a distribution of events concentrated at $\Delta\phi \approx 0$ for photons above an energy threshold close to 2.5 TeV. Therefore, this leads to $\Delta\phi(l^+, l^-) \approx 0$ in leptonic top-quark decay, as well, which is very different from the predictions in the SM [103,104]. This region is poorly understood from a theoretical point of view, though, with SM predictions of a toponium bound state [105] yet to be observed. Furthermore, it is not clear if top quarks arising from photon decay at this energy would still decay preferentially into a W boson and a b quark, as predicted in the SM [106], and a dedicated reconstruction algorithm might be needed. Using this difference of kinematics to constrain LV remains a challenging path in the present state of the theory, but represents an interesting possibility for the future.

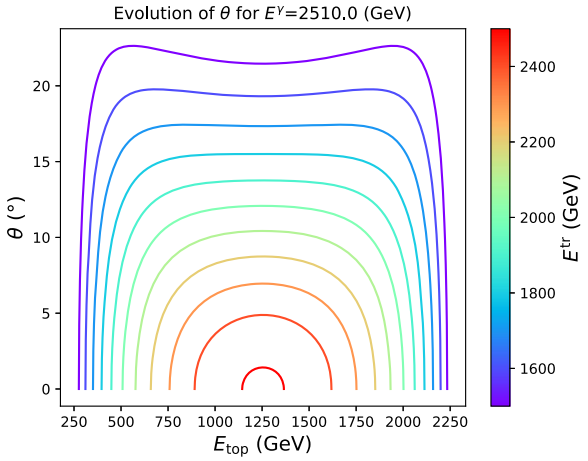

FIG. 3. Opening angles between the final top quarks for a photon energy of 2510 GeV, at different threshold energies.

*d.amram@ip2i.in2p3.fr
†kbouzoud@subatech.in2p3.fr
‡nicolas.pierre.chanon@cern.ch
§hansen@ipnl.in2p3.fr
‖marcosribeiro@usp.br
¶marco.schreck@ufma.br

[1] J. A. Wheeler, On the nature of quantum geometrodynamics, Ann. Phys. (N.Y.) **2**, 604 (1957).
[2] S. W. Hawking, Spacetime foam, Nucl. Phys. **B144**, 349 (1978).
[3] V. A. Kostelecký and S. Samuel, Spontaneous breaking of Lorentz symmetry in string theory, Phys. Rev. D **39**, 683 (1989).
[4] V. A. Kostelecký and S. Samuel, Phenomenological gravitational constraints on strings and higher-dimensional theories, Phys. Rev. Lett. **63**, 224 (1989).
[5] V. A. Kostelecký and S. Samuel, Gravitational phenomenology in higher-dimensional theories and strings, Phys. Rev. D **40**, 1886 (1989).
[6] V. A. Kostelecký and R. Potting, *CPT* and strings, Nucl. Phys. **B359**, 545 (1991).
[7] V. A. Kostelecký and R. Potting, *CPT*, strings, and meson factories, Phys. Rev. D **51**, 3923 (1995).
[8] R. Gambini and J. Pullin, Nonstandard optics from quantum space-time, Phys. Rev. D **59**, 124021 (1999).
[9] M. Bojowald, H. A. Morales-Técotl, and H. Sahlmann, Loop quantum gravity phenomenology and the issue of Lorentz invariance, Phys. Rev. D **71**, 084012 (2005).
[10] G. Amelino-Camelia and S. Majid, Waves on noncommutative space-time and gamma-ray bursts, Int. J. Mod. Phys. A **15**, 4301 (2000).
[11] S. M. Carroll, J. A. Harvey, V. A. Kostelecký, C. D. Lane, and T. Okamoto, Noncommutative field theory and Lorentz violation, Phys. Rev. Lett. **87**, 141601 (2001).
[12] F. R. Klinkhamer and C. Rupp, Spacetime foam, *CPT* anomaly, and photon propagation, Phys. Rev. D **70**, 045020 (2004).
[13] S. Bernadotte and F. R. Klinkhamer, Bounds on length scales of classical spacetime foam models, Phys. Rev. D **75**, 024028 (2007).
[14] S. Hossenfelder, Theory and phenomenology of space-time defects, Adv. High Energy Phys. **2014**, 950672 (2014).
[15] F. R. Klinkhamer, Z-string global gauge anomaly and Lorentz non-invariance, Nucl. Phys. **B535**, 233 (1998).
[16] F. R. Klinkhamer, A *CPT* anomaly, Nucl. Phys. **B578**, 277 (2000).
[17] K. J. B. Ghosh and F. R. Klinkhamer, Anomalous Lorentz and *CPT* violation from a local Chern-Simons-like term in the effective gauge-field action, Nucl. Phys. **B926**, 335 (2018).
[18] P. Hořava, Quantum gravity at a Lifshitz point, Phys. Rev. D **79**, 084008 (2009).
[19] D. Colladay and V. A. Kostelecký, *CPT* violation and the standard model, Phys. Rev. D **55**, 6760 (1997).
[20] D. Colladay and V. A. Kostelecký, Lorentz-violating extension of the standard model, Phys. Rev. D **58**, 116002 (1998).
[21] O. W. Greenberg, *CPT* violation implies violation of Lorentz invariance, Phys. Rev. Lett. **89**, 231602 (2002).
[22] V. A. Kostelecký, C. D. Lane, and A. G. M. Pickering, One-loop renormalization of Lorentz-violating electrodynamics, Phys. Rev. D **65**, 056006 (2002).
[23] D. Colladay and P. McDonald, One-loop renormalization of pure Yang-Mills theory with Lorentz violation, Phys. Rev. D **75**, 105002 (2007).
[24] A. Ferrero and B. Altschul, Renormalization of scalar and Yukawa field theories with Lorentz violation, Phys. Rev. D **84**, 065030 (2011).
[25] E. F. Beall, Measuring the gravitational interaction of elementary particles, Phys. Rev. D **1**, 961 (1970).
[26] S. Coleman and S. L. Glashow, Cosmic ray and neutrino tests of special relativity, Phys. Lett. B **405**, 249 (1997).
[27] G. D. Moore and A. E. Nelson, Lower bound on the propagation speed of gravity from gravitational Čerenkov radiation, J. High Energy Phys. 09 (2001) 023.
[28] R. Lehnert and R. Potting, Čerenkov effect in Lorentz-violating vacua, Phys. Rev. D **70**, 125010 (2004); **70**, 129906(E) (2004).
[29] R. Lehnert and R. Potting, Vacuum Čerenkov radiation, Phys. Rev. Lett. **93**, 110402 (2004).
[30] C. Kaufhold and F. R. Klinkhamer, Vacuum Čerenkov radiation and photon triple-splitting in a Lorentz-non-invariant extension of quantum electrodynamics, Nucl. Phys. **B734**, 1 (2006).
[31] C. Kaufhold and F. R. Klinkhamer, Vacuum Čerenkov radiation in spacelike Maxwell-Chern-Simons theory, Phys. Rev. D **76**, 025024 (2007).
[32] B. Altschul, Vacuum Čerenkov radiation in Lorentz-violating theories without *CPT* violation, Phys. Rev. Lett. **98**, 041603 (2007).
[33] B. Altschul, Cerenkov radiation in a Lorentz-violating and birefringent vacuum, Phys. Rev. D **75**, 105003 (2007).
[34] M. A. Hohensee, R. Lehnert, D. F. Phillips, and R. L. Walsworth, Particle-accelerator constraints on isotropic modifications of the speed of light, Phys. Rev. Lett. **102**, 170402 (2009).
[35] M. A. Hohensee, R. Lehnert, D. F. Phillips, and R. L. Walsworth, Limits on isotropic Lorentz violation in QED from collider physics, Phys. Rev. D **80**, 036010 (2009).
[36] F. R. Klinkhamer and M. Schreck, New two-sided bound on the isotropic Lorentz-violating parameter of modified Maxwell theory, Phys. Rev. D **78**, 085026 (2008).
[37] B. Altschul, Absence of long-wavelength Cerenkov radiation with isotropic Lorentz and *CPT* violation, Phys. Rev. D **90**, 021701(R) (2014).
[38] K. Schober and B. Altschul, No vacuum Cerenkov radiation losses in the timelike Lorentz-violating Chern-Simons theory, Phys. Rev. D **92**, 125016 (2015).
[39] J. S. Díaz and F. R. Klinkhamer, Parton-model calculation of a nonstandard decay process in isotropic modified Maxwell theory, Phys. Rev. D **92**, 025007 (2015).
[40] V. A. Kostelecký and J. D. Tasson, Constraints on Lorentz violation from gravitational Čerenkov radiation, Phys. Lett. B **749**, 551 (2015).

[41] D. Colladay, P. McDonald, and R. Potting, Cherenkov radiation with massive, *CPT*-violating photons, Phys. Rev. D **93**, 125007 (2016).
[42] B. Altschul, Cerenkov-like emission of pions by photons in a Lorentz-violating theory, Phys. Rev. D **93**, 105007 (2016).
[43] D. Colladay, P. McDonald, J. P. Noordmans, and R. Potting, Covariant quantization of *CPT*-violating photons, Phys. Rev. D **95**, 025025 (2017).
[44] D. Colladay, J. P. Noordmans, and R. Potting, Cherenkov-like emission of Z bosons, J. Phys. Conf. Ser. **873**, 012017 (2017).
[45] M. Schreck, Vacuum Cherenkov radiation for Lorentz-violating fermions, Phys. Rev. D **96**, 095026 (2017).
[46] B. Altschul, Why Cerenkov radiation may not occur, even when it is allowed by Lorentz-violating kinematics, Symmetry **9**, 250 (2017).
[47] M. Schreck, Vacuum Cherenkov radiation for Lorentz-violating fermions, J. Phys. Conf. Ser. **952**, 012018 (2018).
[48] M. Schreck, (Gravitational) vacuum Cherenkov radiation, Symmetry **10**, 424 (2018).
[49] F. Duenkel, M. Niechciol, and M. Risse, New bound on Lorentz violation based on the absence of vacuum Cherenkov radiation in ultrahigh energy air showers, Phys. Rev. D **107**, 083004 (2023).
[50] S. Liberati, T. A. Jacobson, and D. Mattingly, High energy constraints on Lorentz symmetry violations, in *Proceedings of the Second Meeting on CPT and Lorentz Symmetry*, V. A. Kostelecký (ed.) (World Scientific Publishing, Singapore, 2001), 10.1142/9789812778123_0036.
[51] T. Jacobson, S. Liberati, and D. Mattingly, TeV astrophysics constraints on Planck scale Lorentz violation, Phys. Rev. D **66**, 081302(R) (2002).
[52] T. Jacobson, S. Liberati, and D. Mattingly, Threshold effects and Planck scale Lorentz violation: Combined constraints from high energy astrophysics, Phys. Rev. D **67**, 124011 (2003).
[53] T. Jacobson, S. Liberati, and D. Mattingly, Lorentz violation at high energy: Concepts, phenomena and astrophysical constraints, Ann. Phys. (Amsterdam) **321**, 150 (2006).
[54] L. Shao and B.-Q. Ma, Lorentz violation effects on astrophysical propagation of very high energy photons, Mod. Phys. Lett. A **25**, 3251 (2010).
[55] B. Altschul, Modeling-free bounds on nonrenormalizable isotropic Lorentz and *CPT* violation in QED, Phys. Rev. D **83**, 056012 (2011).
[56] G. Rubtsov, P. Satunin, and S. Sibiryakov, Calculation of cross sections in Lorentz-violating theories, Phys. Rev. D **86**, 085012 (2012).
[57] P. Satunin, Width of photon decay in a magnetic field: Elementary semiclassical derivation and sensitivity to Lorentz violation, Phys. Rev. D **87**, 105015 (2013).
[58] G. Rubtsov, P. Satunin, and S. Sibiryakov, Prospective constraints on Lorentz violation from ultrahigh-energy photon detection, Phys. Rev. D **89**, 123011 (2014).
[59] T. Kalaydzhyan, Testing gravity on accelerators, in *Proceedings of the Seventh Meeting on CPT and Lorentz Symmetry*, edited by V. A. Kostelecký (World Scientific Publishing, Singapore, 2016), 10.1142/9789813148505_0076.
[60] H. Martínez-Huerta and A. Pérez-Lorenzana, Vacuum Cherenkov radiation and photon decay rates from generic Lorentz invariance violation, J. Phys. Conf. Ser. **761**, 012035 (2016).
[61] H. Martínez-Huerta and A. Pérez-Lorenzana, Restrictions from Lorentz invariance violation on cosmic ray propagation, Phys. Rev. D **95**, 063001 (2017).
[62] H. Martínez-Huerta and A. Pérez-Lorenzana, Photon emission and decay from generic Lorentz invariance violation, J. Phys. Conf. Ser. **866**, 012006 (2017).
[63] H. Martínez-Huerta and A. Pérez-Lorenzana, Effects of Lorentz invariance violation on cosmic ray photon emission and gamma ray decay processes, Proc. Sci. **ICRC2017**, 556 (2018).
[64] F. R. Klinkhamer, M. Niechciol, and M. Risse, Improved bound on isotropic Lorentz violation in the photon sector from extensive air showers, Phys. Rev. D **96**, 116011 (2017).
[65] H. Martínez-Huerta, Lorentz-violation constraints with astroparticle physics, in *Proceedings of the Eighth Meeting on CPT and Lorentz Symmetry*, edited by R. Lehnert (World Scientific Publishing, Singapore, 2019), 10.1142/9789811213984_0034.
[66] P. Satunin, New constraints on Lorentz invariance violation from Crab Nebula spectrum beyond 100 TeV, Eur. Phys. J. C **79**, 1011 (2019).
[67] L. Chen, Z. Xiong, C. Li, S. Chen, and H. He, Strong constraints on Lorentz violation using new γ-ray observations around PeV, Chin. Phys. C **45**, 105105 (2021).
[68] F. Duenkel, M. Niechciol, and M. Risse, Photon decay in ultrahigh-energy air showers: Stringent bound on Lorentz violation, Phys. Rev. D **104**, 015010 (2021).
[69] J.-J. Wei and X.-F. Wu, Tests of Lorentz invariance, arXiv:2111.02029.
[70] V. A. Kostelecký and M. Mewes, Signals for Lorentz violation in electrodynamics, Phys. Rev. D **66**, 056005 (2002).
[71] Q. G. Bailey and V. A. Kostelecký, Lorentz-violating electrostatics and magnetostatics, Phys. Rev. D **70**, 076006 (2004).
[72] V. A. Kostelecký and M. Mewes, Cosmological constraints on Lorentz violation in electrodynamics, Phys. Rev. Lett. **87**, 251304 (2001).
[73] V. A. Kostelecký and M. Mewes, Electrodynamics with Lorentz-violating operators of arbitrary dimension, Phys. Rev. D **80**, 015020 (2009).
[74] F. Kislat, Constraints on Lorentz invariance violation from optical polarimetry of astrophysical objects, Symmetry **10**, 596 (2018).
[75] A. S. Friedman, D. Leon, K. D. Crowley, D. Johnson, G. Teply, D. Tytler, B. G. Keating, and G. M. Cole, Constraints on Lorentz invariance and *CPT* violation using optical photometry and polarimetry of active galaxies BL Lacertae and S5 B0716 + 714, Phys. Rev. D **99**, 035045 (2019).
[76] A. S. Friedman, R. Gerasimov, D. Leon, W. Stevens, D. Tytler, B. G. Keating, and F. Kislat, Improved constraints on anisotropic birefringent Lorentz invariance and *CPT*

violation from broadband optical polarimetry of high redshift galaxies, Phys. Rev. D **102**, 043008 (2020).
[77] R. Gerasimov, P. Bhoj, and F. Kislat, New constraints on Lorentz invariance violation from combined linear and circular optical polarimetry of extragalactic sources, Symmetry **13**, 880 (2021).
[78] Ch. Eisele, A. Yu. Nevsky, and S. Schiller, Laboratory test of the isotropy of light propagation at the 10^{-17} level, Phys. Rev. Lett. **103**, 090401 (2009).
[79] S. Herrmann, A. Senger, K. Möhle, M. Nagel, E. V. Kovalchuk, and A. Peters, Rotating optical cavity experiment testing Lorentz invariance at the 10^{-17} level, Phys. Rev. D **80**, 105011 (2009).
[80] M. A. Hohensee, P. L. Stanwix, M. E. Tobar, S. R. Parker, D. F. Phillips, and R. L. Walsworth, Improved constraints on isotropic shift and anisotropies of the speed of light using rotating cryogenic sapphire oscillators, Phys. Rev. D **82**, 076001 (2010).
[81] T. Zhang, J. Bi, Y. Zhi, J. Peng, L. Li, and L. Chen, Test of Lorentz invariance using rotating ultra-stable optical cavities, Phys. Lett. A **416**, 127666 (2021).
[82] V. A. Kostelecký and N. Russell, Data tables for Lorentz and *CPT* violation, Rev. Mod. Phys. **83**, 11 (2011).
[83] Z. Cao *et al.* (LHAASO Collaboration), Ultrahigh-energy photons up to 1.4 petaelectronvolts from 12 γ-ray galactic sources, Nature (London) **594**, 33 (2021).
[84] Z. Cao *et al.* (LHAASO Collaboration), An ultrahigh-energy γ-ray bubble powered by a super PeVatron, Sci. Bull. **69**, 449 (2024).
[85] M. Unger, G. R. Farrar, and L. A. Anchordoqui, Origin of the ankle in the ultrahigh energy cosmic ray spectrum, and of the extragalactic protons below it, Phys. Rev. D **92**, 123001 (2015).
[86] J. Ellis, N. E. Mavromatos, D. V. Nanopoulos, A. S. Sakharov, and E. K. G. Sarkisyan, Robust limits on Lorentz violation from gamma-ray bursts, Astropart. Phys. **25**, 402 (2006); [Astropart. Phys. **29(E)**, 158 (2008)].
[87] Z. Chang, Y. Jiang, and H.-N. Lin, A unified constraint on the Lorentz invariance violation from both short and long GRBs, Astropart. Phys. **36**, 47 (2012).
[88] ATLAS Collaboration, Measurement of the inclusive isolated-photon cross section in pp collisions at $\sqrt{s} =$ 13 TeV using 36 fb^{-1} of ATLAS data, J. High Energy Phys. 10 (2019) 203.
[89] CMS Collaboration, Measurement of differential cross sections for inclusive isolated-photon and photon + jet production in proton-proton collisions at $\sqrt{s} = 13$ TeV, Eur. Phys. J. C **79**, 20 (2019).
[90] E. Bothmann *et al.* (Sherpa), Event generation with SHERPA2.2, SciPost Phys. **7**, 034 (2019).
[91] F. Siegert, A practical guide to event generation for prompt photon production with Sherpa, J. Phys. G **44**, 044007 (2017).
[92] ATLAS Collaboration (2020), Measurement of the inclusive isolated-photon cross section in pp collisions at $\sqrt{s} = 13$ TeV using 36 fb^{-1} of ATLAS data. HEPData (collection), 10.17182/hepdata.91968.
[93] C. Bierlich, A. Buckley, J. Butterworth, C. H. Christensen, L. Corpe, D. Grellscheid, J. F. Grosse-Oetringhaus, C. Gutschow, P. Karczmarczyk, J. Klein *et al.*, Robust independent validation of experiment and theory: Rivet version 3, SciPost Phys. **8**, 026 (2020).
[94] ATLAS Collaboration, Measurement of the inclusive isolated prompt photon cross section in pp collisions at $\sqrt{s} = 8$ TeV with the ATLAS detector, J. High Energy Phys. 08 (2016) 005.
[95] ATLAS Collaboration, CERN-LHCC-2010-013.
[96] A. L. Read, Presentation of search results: The CL_s technique, J. Phys. G **28**, 2693 (2002).
[97] D0 Collaboration, Measurement of the differential cross section for the production of an isolated photon with associated jet in $p\bar{p}$ collisions at $\sqrt{s} = 1.96$ TeV, Phys. Lett. B **666**, 435 (2008).
[98] Y. Ohnishi, T. Abe, T. Adachi, K. Akai, Y. Arimoto, K. Ebihara, K. Egawa, J. Flanagan, H. Fukuma, Y. Funakoshi *et al.*, Accelerator design at SuperKEKB, Prog. Theor. Exp. Phys. **2013**, 03A011 (2013).
[99] FCC Collaboration, FCC-ee: The lepton collider. Future Circular Collider conceptual design report volume 2, Eur. Phys. J. ST **228**, 261 (2019).
[100] FCC Collaboration, FCC-hh: The hadron collider. Future Circular Collider conceptual design report volume 3, Eur. Phys. J. ST **228**, 755 (2019).
[101] M. S. Berger, V. A. Kostelecký, and Z. Liu, Lorentz and *CPT* violation in top-quark production and decay, Phys. Rev. D **93**, 036005 (2016).
[102] A. Carle, N. Chanon, and S. Perriès, Prospects for Lorentz invariance violation searches with top pair production at the LHC and future hadron colliders, Eur. Phys. J. C **80**, 128 (2020).
[103] CMS Collaboration, Measurement of the top quark polarization and $t\bar{t}$ spin correlations using dilepton final states in proton-proton collisions at $\sqrt{s} = 13$ TeV, Phys. Rev. D **100**, 072002 (2019).
[104] ATLAS Collaboration, Inclusive and differential cross-sections for dilepton $t\bar{t}$ production measured in $\sqrt{s} =$ 13 TeV pp collisions with the ATLAS detector, J. High Energy Phys. 07 (2023) 141.
[105] B. Fuks, K. Hagiwara, K. Ma, and Y.-J. Zheng, Signatures of toponium formation in LHC run 2 data, Phys. Rev. D **104**, 034023 (2021).
[106] B. Altschul, Top hadrons in Lorentz-violating field theory, Phys. Rev. D **102**, 075010 (2020).